



Rho, a Fraction From *Rhodiola crenulate*, Ameliorates Hepatic Steatosis in Mice Models

Qin Yi^{1†}, Puyang Sun^{1†}, Juan Li¹, Siming Kong¹, Jinying Tian¹, Xuechen Li¹, Yanan Yang², Peicheng Zhang², Yuying Liu³, Jingyan Han³, Xiaolin Zhang^{1*} and Fei Ye^{1*}

¹ Beijing Key Laboratory of New Drug Mechanisms and Pharmacological Evaluation Study, Institute of Materia Medica, Chinese Academy of Medical Science & Peking Union Medical College, Beijing, China, ² State Key Laboratory of Bioactive Substance and Function of Natural Medicines, Institute of Materia Medica, Chinese Academy of Medical Science & Peking Union Medical College, Beijing, China, ³ Tasly Microcirculation Research Center, Peking University Health Science Center, Beijing, China

OPEN ACCESS

Edited by:

Vincenzo Lionetti,
Sant'Anna School of Advanced
Studies, Italy

Reviewed by:

Claudia Kusmic,
Istituto di Fisiologia Clinica (CNR), Italy
Giuseppe Calamita,
Università degli Studi di Bari Aldo
Moro, Italy

*Correspondence:

Xiaolin Zhang
zhangxiaolin@imm.ac.cn
Fei Ye
yefei@imm.ac.cn

†Co-first authors.

Specialty section:

This article was submitted to
Vascular Physiology,
a section of the journal
Frontiers in Physiology

Received: 12 October 2017

Accepted: 28 February 2018

Published: 14 March 2018

Citation:

Yi Q, Sun P, Li J, Kong S, Tian J, Li X,
Yang Y, Zhang P, Liu Y, Han J,
Zhang X and Ye F (2018) *Rho*, a
Fraction From *Rhodiola crenulate*,
Ameliorates Hepatic Steatosis in Mice
Models. *Front. Physiol.* 9:222.
doi: 10.3389/fphys.2018.00222

The prevalence of non-alcoholic fatty liver disease (NAFLD), which is developed from hepatic steatosis, is increasing worldwide. However, no specific drugs for NAFLD have been approved yet. To observe the effects of *Rho*, a fraction from *Rhodiola crenulate*, on non-alcoholic hepatic steatosis, three mouse models with characteristics of NAFLD were used including high-fat diet (HFD)-induced obesity (DIO) mice, KKAY mice, and HFD combined with tetracycline stimulated Model-T mice. Hepatic lipid accumulation was determined via histopathological analysis and/or hepatic TG determination. The responses to insulin were evaluated by insulin tolerance test (ITT), glucose tolerance test (GTT), and hyperinsulinemic-euglycemic clamp, respectively. The pathways involved in hepatic lipid metabolism were observed via western-blot. Furthermore, the liver microcirculation was observed by inverted microscopy. The HPLC analysis indicated that the main components of *Rho* were flavan polymers. The results of histopathological analysis showed that *Rho* could ameliorate hepatic steatosis in DIO, KKAY, and Model-T hepatic steatosis mouse models, respectively. After *Rho* treatment in DIO mice, insulin resistance was improved with increasing glucose infusion rate (GIR) in hyperinsulinemic-euglycemic clamp, and decreasing areas under the blood glucose-time curve (AUC) in both ITT and GTT; the pathways involved in fatty acid uptake and *de novo* lipogenesis were both down-regulated, respectively. However, the pathways involved in beta-oxidation and VLDL-export on hepatic steatosis were not changed significantly. The liver microcirculation disturbances were also improved by *Rho* in DIO mice. These results suggest that *Rho* is a lead nature product for hepatic steatosis treatment. The mechanism is related to enhancing insulin sensitivity, suppressing fatty acid uptake and inhibiting *de novo* lipogenesis in liver.

Keywords: a fraction from *Rhodiola crenulate* (*Rho*), non-alcoholic fatty liver disease (NAFLD), hepatic steatosis, insulin resistance, hepatic lipid metabolism

INTRODUCTION

Non-alcoholic fatty liver disease (NAFLD), a spectrum of liver disease developing progressively from simple steatosis to steatohepatitis, fibrosis, and cirrhosis, is increasing worldwide with the incidence of 20–30% in Western countries and 5–18% in Asia (Sayiner et al., 2016) and is caused by a multitude of factors including the insulin resistance (Bugianesi et al., 2010; Petta et al., 2016). In normal conditions, insulin inhibits the lipolysis of white adipose tissue and gluconeogenesis of liver, but promotes hepatic lipogenesis; in insulin-resistant states, usually, the inhibitions of lipolysis and gluconeogenesis are failed, but the promotion of lipogenesis is preserved (Gruben et al., 2014). As a result, the auxo-action of insulin resistance in hepatic steatosis/NASH is induced by enhancing *de novo* lipogenesis in liver and subsequent lipolysis in adipose tissue. Therefore, insulin resistance plays a key role in the progression of NAFLD and maybe a therapeutic target for its treatment.

Vitamin E and pioglitazone currently remain the first line off label drugs for NASH. Several agents are currently in intermediate or advanced stages of development, however, no specific drugs for NAFLD have been approved yet (Banini and Sanyal, 2017). Here, we identified *Rho*, the active fractions from *Rhodiola crenulata*, as an effective nature product for NAFLD treatment. *Rhodiola crenulata* has been used for the treatment of cardiovascular disease for more than one thousand years in China. It is classified to *Crassulaceae* family, and contains phenols, flavonoids, and other compounds, which produce antioxidant, anti-inflammatory, antidepressant, anti-fatigue, cardiac protection, neuroprotection, and anti-lipogenesis effects (Wu et al., 2009; Chan, 2012; Grech-Baran et al., 2015). In this study, we demonstrated that *Rho* could improve hepatic steatosis in three NAFLD animal models. Moreover, its mechanism, including the insulin sensitizing effect and the pathways involved in hepatic lipid metabolism, was investigated in DIO mice.

METHODS

Preparation of Active Fractions From *Rhodiola crenulata* (*Rho*)

The roots of *R. crenulata* were collected in October 2010 from Shannan Tibet Autonomous Region, and identified by Prof. Lin Ma (Institute of Materia Medica, Peking Union Medical College and Chinese Academy of Medical Sciences, Beijing, China). Its voucher specimen was deposited in the Herbarium of the Department of Medicinal plants, Institute of Materia Medica, Chinese Academy of Medical Sciences and Peking Union Medical College, Beijing, P. R. China.

Dried roots (100 kg) of *R. crenulata* were extracted with 80% EtOH for three times. After the solvent was evaporated under reduced pressure, the residue was resuspended in H₂O (50 L) for 24 h. The deposits were filtered from the solution. Then, the aqueous layer (18 Kg) was concentrated under reduced pressure, and applied to a HP-20 macroporous adsorbent resin (40 Kg, dried weight) column. Successive elution from the column with H₂O (RC-1), 15% EtOH (RC-2), 30% EtOH (RC-3), 50% EtOH

(RC-4), 70% EtOH (RC-5), and finally 95% EtOH (RC-6) yielded five corresponding fractions after removing solvents.

The chemical constituents of the prepared RC-3 were analyzed by high-performance liquid chromatography (HPLC) consisting of a quaternary delivery system, an auto-sampler, and a diode array detector (DAD). The analysis was performed on an Apollo C18 (250 mm × 4.6 mm, 5 μm) column using the mixture of methanol (A) and 0.2% acetic acid (B) as mobile phase in an elution program (0–30 min, 5% A to 15% A; 30–60 min, 15% A; 60–80 min, 15% A to 25% A; 80–90 min, 25% A to 100% A; 90–100 min, 100% A). The flow rate was 1.0 ml/min and the chromatogram was recorded at 280 nm.

Chemicals and Reagents

Fenofibrate (Feno) from Fournier Pharma (France); Fluvastatin (Flu) from Beijing Novartis Pharma Ltd; Tetracycline was purchased from AMRESCO (USA); Polyene Phosphatidylcholine (PPC) from Sanofi, Beijing (China); Rosiglitazone (Rosi) from GSK, China; Anti-β-actin antibody, anti-FAS antibody, anti-ACC antibody from Cell Signaling Technology (USA); anti-MTTP antibody, anti-CPT-1 antibody, anti-CD36 antibody from Abcam (USA); anti-SREBP-1c antibody from SANTA (USA); commercial kits for liver triglyceride, ECL reactions from Applygen Technologies Inc.

Animal and Diets

All animals were purchased from the Animal Center of Institute of Laboratory Animal Sciences, CAMS & PUMC, and grouped housed (four mice per cage) in grommet cages under the condition of temperature 21~23°C, humidity 40~60%, 12 h light/dark cycle, *ad libitum* access to water and chow diet. Efforts were made to minimize animal suffering. All animal experiments were performed in accordance with the guidelines established by the National Institutes of Health for the care and use of laboratory animals and were approved by the Animal Care Committee of CAMS & PUMC.

The DIO mice were induced by HFD (containing 50% fat, 36% carbohydrate, and 14% protein in energy) in male 4 weeks C57BL/6 mice. After a 12-week induction, mice with body weight >40 g were selected and randomly divided into three groups ($n = 8$): the DIO group, Positive drug group (Feno, 100 mg/kg body weight/d; or Flu, 50 mg/kg body weight/d; or Rosi, 8 mg/kg body weight/d), and *Rho* treatment group (200 mg/kg body weight/d). Meanwhile, aged-matched mice fed with the standard chow diet (containing 12% fat, 62% carbohydrate, and 26% protein in energy) were used as normal control (Con).

The male KKAY mice, which were 11 weeks old with the average weight about 35 g, were fed chow diet (1K65, Beijing HFK Bioscience Co. Ltd., China), and randomly divided into three groups ($n = 8$): model control KKAY, PPC-K, and *Rho*-K; and orally treated with water, PPC (200 mg/kg body weight/d), and *Rho* (400 mg/kg body weight/d), respectively.

Model-T mice were induced with HFD for 11 weeks and then intraperitoneally injected with tetracycline (50 mg/kg body weight/d) for 17 days in male 4 weeks old C57BL/6 mice. The model mice were also divided into three groups ($n = 8$): the model control Model-T, PPC-T, and *Rho*-T; administrated with

water, PPC (200 mg/kg body weight/d), and *Rho* (200 mg/kg body weight/d), respectively. Aged-matched mice fed with the standard chow diet were used as normal control (Con-T).

Insulin Sensitivity Evaluation

Insulin tolerance test (ITT) and intraperitoneal glucose tolerance test (IPGTT) were performed as previously described (Tian et al., 2015). Briefly, mice were fasted for 2 h. Blood samples were collected from tails for determination of baseline values of blood glucose ($t = 0$ min). The mice were then subcutaneous injected with insulin 0.27 U/kg or intraperitoneal injected with glucose 1 g/kg, then blood samples were collected at 30, 60, 120 min for glucose measurement. The levels of blood glucose were measured by a glucose oxidase (GOD) method. The values of area under the glucose-time curve (AUC) were calculated.

The hyperinsulinemic-euglycemic clamp test was conducted according to a protocol previously published (Ye et al., 2008). Briefly, after fasting for 4 h, the serum insulin level of mouse was clamped by injecting insulin at 60 pmol/kg/min rates, meanwhile, its homeostatic blood glucose was maintain at normal physiological level by infusing 10% glucose at the different rates. The glucose infusion rate (GIR) was calculated when the blood glucose was maintained at 95 ± 5 mg/dl for more than 20 min.

Histological Analysis of Liver

After 5 weeks of treatment for DIO mice, 8 weeks of treatment for KKAY mice, 6 weeks of treatment for Model-T mice, mice were sacrificed after a 16-h fasting. Liver tissues were dissected quickly on ice. Parts of them (the left middle lobe) were immediately fixed in 4% paraformaldehyde, paraffin embedded, and then stained with hematoxylin and eosin. Hepatic steatosis was graded on the basis of the semiquantitative scoring system as previously described (Ma et al., 2011).

Determination of Triglyceride Content in Liver

After 5 weeks of treatment for DIO mice, TG content were determined, the Left lateral lobe was collected. The TG content of liver were extracted according to the method published previously (Bligh and Dyer, 1959), and determined with the commercial biochemical kits (Jian Cheng Bioengineering Institute, Nanjing, China).

Western-Blot Analysis

After 5 weeks of treatment for DIO mice, livers were homogenized in ice-cold buffer (containing 50 mM HEPES, 10 mM sodium pyrophosphate, 100 mM sodium fluoride, 2 mM sodium orthovanadate, 1% NP-40, 4 mM EDTA, and 2 mM PMSE, pH 7.4). Western blotting was performed to determine the pathways related to hepatic lipid metabolism as previously described (Ma et al., 2011). The gel image analysis system (Fluorochem 5500, Alpha Innotech, USA) was used for the images acquisition.

Determination of Microcirculatory Parameters

The hepatic microcirculation in DIO mice was observed with stereomicroscope (DM-IRB, Leica, Germany), and recorded with a color camera (JK-TU53H, 3CCD camera, Toshiba, Japan) and a DVD recorder (DVR-R25, Malata, China), respectively, as the method previously described (Chen et al., 2008).

Statistical Methods

The data were analyzed by one-way ANOVA analysis. All values are presented as means \pm SD, and statistical significance was set at a value of $P < 0.05$.

RESULTS

Analysis of Chemical Constituents in *Rho*

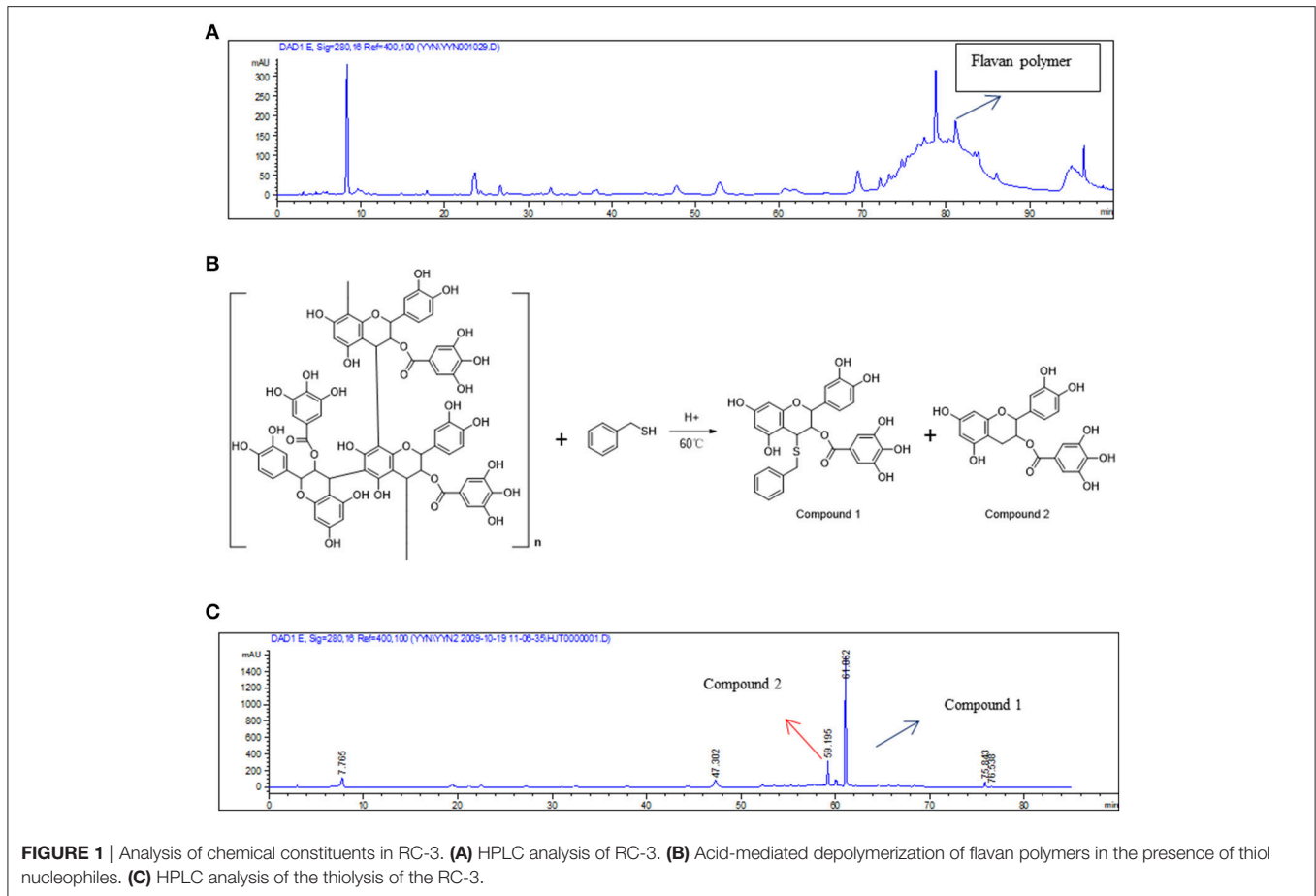
The results indicated that the main components of the RC-3 are flavan polymers (Figure 1A). A literature (Thompson et al., 1972) search revealed that acid-mediated depolymerization of flavan polymers in the presence of thiol nucleophiles leads to β -C-4 substituted flavanol derivatives (Figure 1B). Hence, the main contents of RC-3 were confirmed as flavan polymers by using the reported method. The analysis of the thiolysis of RC-3 was performed by the same HPLC method with that of RC-3 (Figure 1C).

Rho Ameliorates Hepatic Steatosis in 3 Animal Models

The hepatic steatosis in DIO mice was induced by long-term *ad libitum* feeding of HFD which contents much higher fat (50%) compared with the chow diet (12%). In this manner, the process of hepatic steatosis reflects well the clinical cases (Cong et al., 2008). The DIO mice displayed marked macrovesicular and microvesicular steatosis in liver (Figure 2A). Semiquantitative scoring result showed that the score of the DIO mice was 2.1-fold increased compared with that of Con mice (Figure 2D). The hepatic steatosis was significantly improved by *Rho* treatment with 35.5% reduction in lipid accumulation compared with DIO mice (Figures 2A,D). The hepatic TG content in DIO mice was 6.5-fold increased compared with that in Con mice. Notably, the elevated TG content was decreased by 35.8% in *Rho* treatment group (Figure 2E).

The KKAY mice are typical T2DM animal model with obese, hyperglycemic, hyperinsulinemic, insulin resistant, and obvious hepatic steatosis (Yamamoto et al., 2010). KKAY mice exhibited obvious hepatic steatosis with hepatocyte lipidosis throughout the entire lobule, and the hepatic cords structure was not clear (Figure 2B). After 8 weeks *Rho* treatment, the elevated hepatocyte lipidosis was completely ameliorated with 33.3% decrease in the hepatic steatosis scores compared with that in KKAY mice (Figures 2B,D).

Model-T is an animal model of drug-induced hepatotoxicity and steatosis (Heaton et al., 2007; Brüning et al., 2014). It is found that tetracycline can induce hepatic microvesicular steatosis, which is severe and even fatal in some vulnerable patients, by regulating the expressions of the genes associated with lipid metabolism, such as increased biosynthesis of TG and



cholesterol, decreased β -oxidation of fatty acids (Bhagavan et al., 1982; Yin et al., 2006). In Model-T mice, the lobules displayed severe lipidosis and ballooning degeneration (**Figure 2C**). *Rho* treatment significantly ameliorated the steatosis and hepatocyte swelling. The steatosis score in Model-T group was significantly increased compared with that in Con-T group, and decreased by 25% after *Rho* treatment (**Figure 2D**).

Rho Improves Insulin Resistance in DIO Mice

Glucose infusion rate (GIR) in hyperinsulinemic-euglycemic clamp test is the recognized gold index for the evaluation of insulin sensitivity *in vivo*. In our studies, the GIR value in DIO mice was 79.9% lower than that in Con mice. After 3 weeks of treatment, GIR was increased by 141.1, 158.7, and 108.7% in Rosi, Feno, and *Rho* group, respectively, compared with that in DIO group (**Figure 3A**).

Furthermore, to evaluate the insulin sensitizing effect of *Rho*, ITT and IPGTT were conducted at day 22 and day 25, respectively. DIO mice exhibited a higher level of glucose in response to insulin and glucose load (**Figures 3C,E**). The two parameters, AUC-ITT (area under the curve in ITT) and AUC-IPGTT (area under the curve in IPGTT) were both much higher in DIO mice than those of control mice (**Figures 3D,F**). *Rho*

administration suppressed the elevated glucose levels both in ITT and IPGTT (**Figures 3C,E**). Consistently, the elevated AUC-ITT and AUC-IPGTT was reduced by 18.9% and 15.5%, respectively (**Figures 3D,F**).

The FPI (fasting plasma insulin) was also determined to evaluate the insulin sensitizing effect of *Rho*. As shown in **Figure 3B**, DIO mice displayed notable hyperinsulinemia compared to Con mice; *Rho* treatment decreased the FPI significantly and had comparable effects with the positive drug.

Rho Ameliorates Hepatic Microcirculation Disturbances in DIO Mice

The hepatic microcirculation was observed by inverted microscopy, the central venular diameter, sinusoids perfusion, velocities of RBCs and shear rate of RBCs in central veins area were estimated, respectively. As shown in **Figure 4**, *Rho* could ameliorate the hepatic microcirculation disturbances. The narrowed central vein diameter in DIO mice was expanded by 14.9% after *Rho* treatment (**Figures 4A,B**). Compared with Con mice, the number of perfused sinusoids in central veins area was 64.6% decreased in DIO mice; after *Rho* treatment it was increased by 67.6% compared with that in DIO mice (**Figures 4C,D**). The RBCs velocity and share rates in central veins area were also enhanced by *Rho* treatment, and the

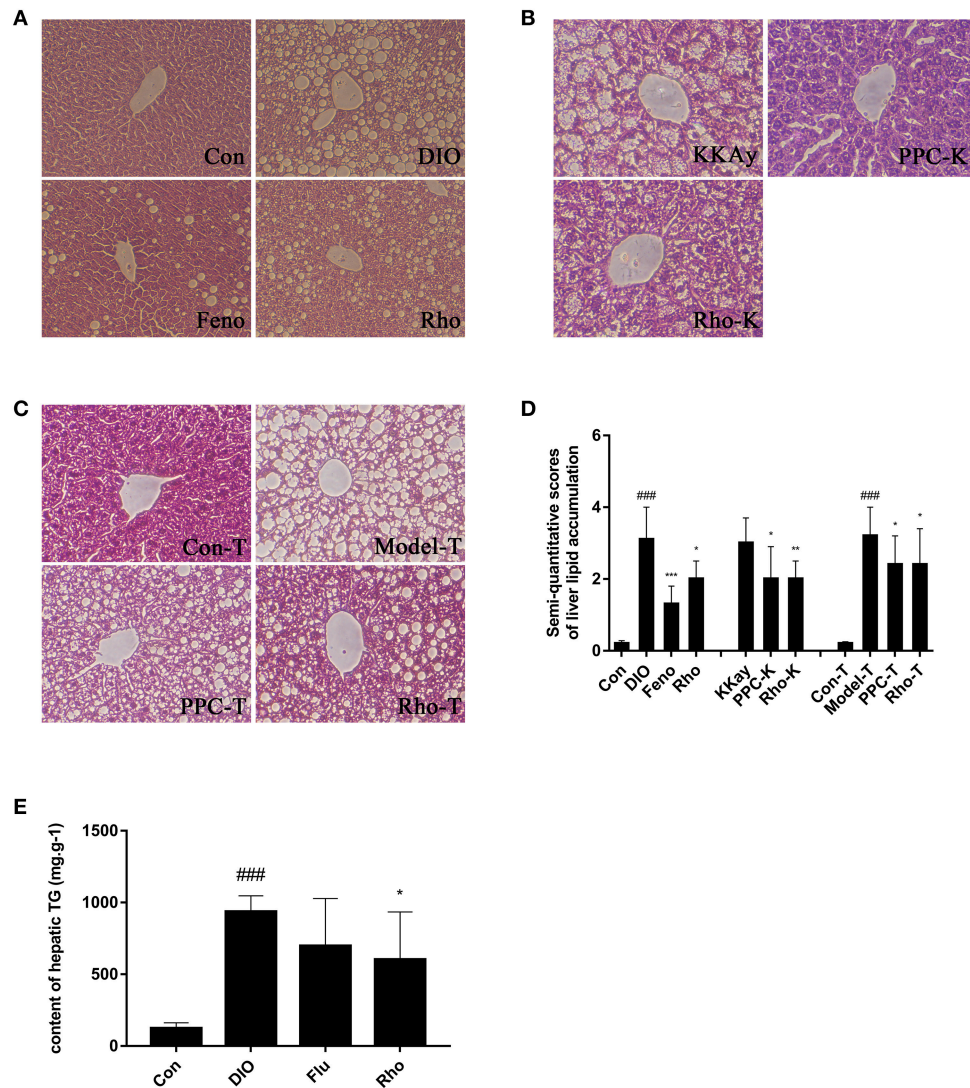


FIGURE 2 | The effect of *Rho* on hepatic steatosis. **(A)** Liver histopathological analysis in DIO mice. **(B)** Liver histopathological analysis in KKAY mice. **(C)** Liver histopathological analysis in high-fat diet combined with tetracycline-induced Model-T mice. (H&E stained) **(D)** Semi-quantitative scoring of steatosis. **(E)** Hepatic triglyceride content. ### $p < 0.001$ vs. normal control group; * $p < 0.05$, ** $p < 0.01$, *** $p < 0.001$, vs. model control group, respectively, $n = 8$.

enhancement was 55.3 and 32.9% compared with that in DIO mice, respectively (Figures 4E,F).

Rho Changes Pathways Involved in Hepatic Lipid Metabolism in DIO Mice

After 5 weeks of *Rho* treatment in DIO mice, the pathways involved in hepatic lipid metabolism including uptake, lipogenesis, oxidation and export were evaluated by Western Blot. As shown in Figure 5, the expression of CD36, SREBP-1c, FAS, ACC, CPT-1, and MTP was up-regulated in livers of DIO mice, which indicated that the 4 pathways were all enhanced by HFD inducement. Remarkably, the pathways involved in fatty acid uptake and *de novo* lipogenesis were both down-regulated by *Rho* treatment with decreased expression of CD36, FAS, and

ACC. However, the pathways involved in beta-oxidation and VLDL-export on hepatic steatosis were not changed significantly without changing the protein level of CPT-1 and MTP.

DISCUSSION

Numerous studies have shown that *R. crenulata* has neuroprotective, anti-tumor, anti-inflammatory, anti-depression, anti-fatigue, immune regulation, and other effects (Lekomtseva et al., 2017; Wei et al., 2017). Lin et al. indicated that *R. crenulata* root extract (RCE), which contained 3.5% salidroside, regulated hepatic glycogen, and lipid metabolism *in vitro* (HepG2 cells) and *in vivo* (SD rats) via activation of the AMPK pathway (Lin et al., 2016). These results suggest that RCE is a potential

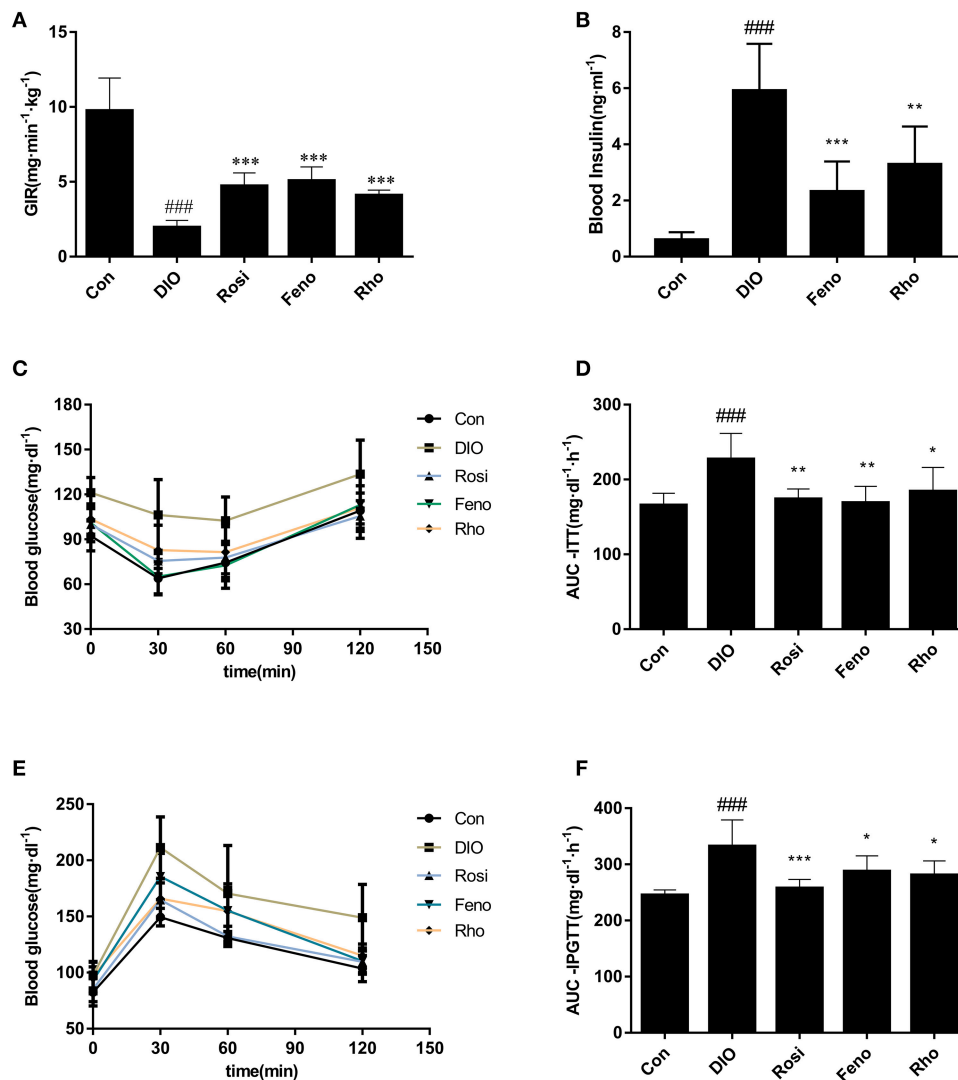


FIGURE 3 | Effects of *Rho* on insulin resistance in high-fat-diet induced DIO mice. **(A)** Values of GIR in hyperinsulinemic-euglycemic clamp test. The DIO mice were administrated with *Rho* (200 mg/kg) for 20 days. Both rosiglitazone (Rosi, 10 mg/kg) and fenofibrate (Feno, 10 mg/kg) were used as the positive control. After fasting for 4 h, the animals were infused insulin at 60 pmol/kg/min rates and 10% glucose at different rates for clamping the level of blood glucose at 95 ± 5 mg/dl. **(B)** Changes of fasting plasma insulin. **(C)** Changes of blood glucose levels in ITT. **(D)** Values of AUC-ITT. **(E)** Changes of blood glucose in IPGTT. **(F)** Values of AUC-IPGTT, $n = 8$. ### $p < 0.001$ vs. Con; * $p < 0.05$, ** $p < 0.01$, *** $p < 0.001$ vs. DIO.

intervention for patients with NAFLD. However, this inference is not reliable because the animal model used in this study did not have lipid accumulation in the liver, and the SD rats were fed RCE just for 3 days. David Vauzour et al. indicated that n-3 Fatty acids combined with flavan-3-ols (FLAV) prevent steatosis and liver injury in a murine model by regulating the expression of genes involved in hepatic lipid accumulation, such as PPAR α (Vauzour et al., 2018). FLAV, a class of plant bioactive flavonoid compounds found in cocoa, tea, and berries, were found to have the effects of insulin sensitizing, antioxidant and anti-inflammation, and used as an emerging dietary strategy for NAFLD prevention (Rodriguez-Ramiro et al., 2016). In our study, the HPLC analysis indicated that the main components

of *Rho* were flavan polymers. *Rho* ameliorated hepatic steatosis in three NAFLD mice models including high-fat diet-induced DIO mice, KKAY mice, and HFD combined with tetracycline stimulated Model-T mice. These results suggest that *Rho* is a lead nature product for NAFLD treatment.

***Rho* Decreased the Uptake of Free Fatty Acids via Down-Regulating the Expression of CD36 in the Liver of DIO Mice**

In steatosis, the early stage of NAFLD, the imbalance between lipid storage and lipid removal in the liver results in the triacylglycerols (TAGs) accumulation (Bugianesi et al., 2010).

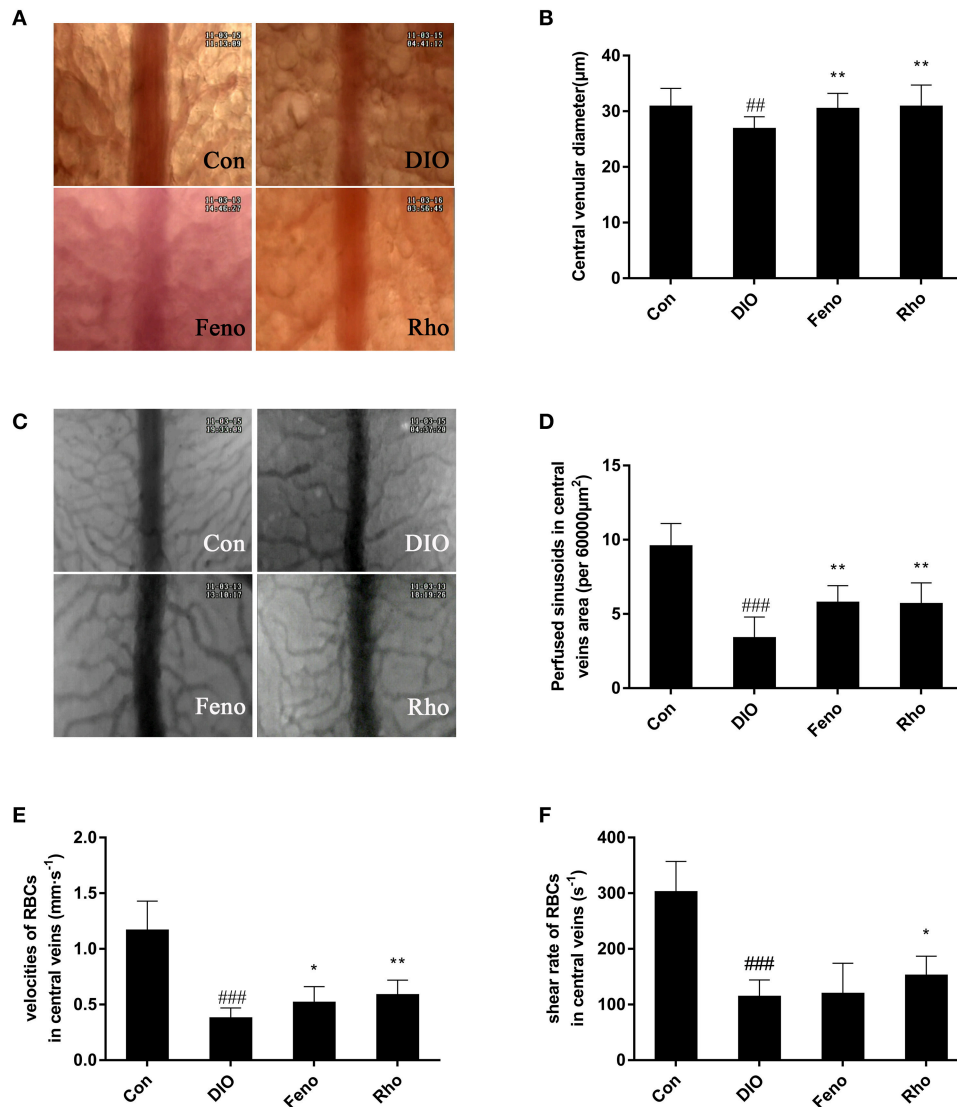
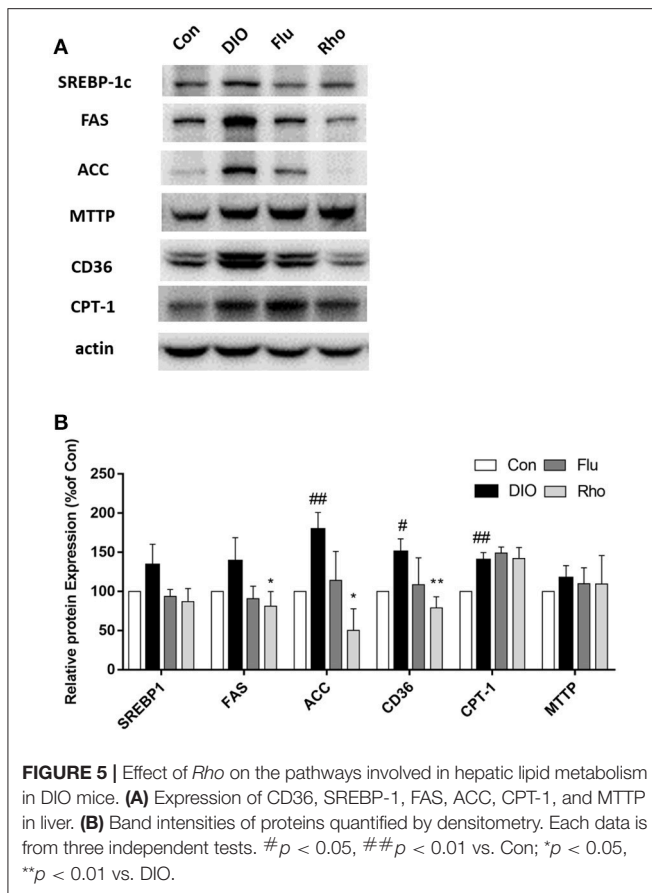


FIGURE 4 | Effects of *Rho* on hepatic microcirculation disturbances in DIO mice. **(A)** Representative images of central venular diameter ($\times 200$). **(B)** Central venular diameter. **(C)** Representative images of sinusoids of central veins area ($\times 200$). **(D)** Perfused sinusoids in the central veins area (per field). **(E)** The velocity of RBCs in central veins. **(F)** Shear rates of RBCs in central veins. Data are shown as the means \pm SD. $^{##}p < 0.01$, $^{###}p < 0.001$ vs. Con; $^{*}p < 0.05$, $^{**}p < 0.01$ vs. DIO, $n = 8$.

The lipid storage mainly derived from the uptake of free fatty acids and *de novo* synthesis within the liver. The lipid removal is mainly derived from fatty acid oxidation in the mitochondria and the VLDL export. CD36 is an important membrane protein for FFAs uptake. The up-regulated expression of CD36 was observed in some pathological conditions such as obesity, diabetes and non-alcoholic fatty liver disease, resulted in the increasing uptake of free fatty acids into the liver (Koonen et al., 2007). Miqulena-Colina ME et al. showed that overexpression of CD36 is strongly associated with insulin resistance (Miqulena-Colina et al., 2011). In this study, the hepatic expression of CD36 in DIO mice was raised. *Rho* treatment reduced the expression of CD36, thus reduced the intake of liver fatty acids and

improved lipid accumulation in the liver. Though the detail mechanism between insulin resistance and CD36 expression is still unknown, the down-regulation of CD36 might be relate to the improvement of insulin resistance. Carnitine palmitoyl transferase 1 (CPT1) is the key factor in fatty acid oxidation in the mitochondria (Orellana-Gavaldà et al., 2011). The human microsomal triglyceride transfer protein (MTTP) carries lipid transfer function to remove lipid from liver by the assembly and secretion of very-low-density lipoprotein (VLDL) (Pereira et al., 2011). In DIO mice, the CPT1 expression was up-regulated, and there were no changes observed in the MTTP expression. *Rho* treatment did not affect the expression of the two proteins mentioned above. These results indicated that the pathways



involved in beta-oxidation and VLDL-export on hepatic steatosis were not changed significantly after *Rho* treatment. Usually, hepatic lipogenesis means TG synthesized from the esterification of free fatty acids (FFA) with glycerol-3-phosphate (Rodríguez et al., 2006). Glycerol-3-phosphate derives from three metabolic sources: (1) glucose from glycolysis; (2) lipolysis-derived glycerol; and (3) glycerol uptake mediated by AQP9 (Rodríguez et al., 2011; Calamita et al., 2012), which expresses lower during NAFLD in patients and in murine models (Gena et al., 2013; Rodríguez et al., 2014). The down-regulated expression of AQP9 may be a compensatory mechanism to decrease the *de novo* TG synthesis. Sexual dimorphism in hepatocyte glycerol permeability might be a significant cause for their different prevalence of insulin resistance and NAFLD (Rodríguez et al., 2015). The change of the AQP9 and the gender difference was not observed in this study. These issues should be addressed in the future.

***Rho* Decreased the *de Novo* Lipogenesis via Down-Regulating the Expression of SREBP-1c, FAS, and ACC in the Liver of DIO Mice**

The expressions of SREBP-1c, FAS, and ACC in the liver affect the hepatic *de novo* synthesis. SREBP-1c is considered the major

mediator for the insulin-regulated lipogenesis. It is up-regulated in NAFLD and plays an important role in the lipid accumulation in fatty liver (Ferre and Foufelle, 2010). In our study, the hepatic expression of SREBP-1c in the DIO mice was significantly higher than that in Con mice. *Rho* had a tendency to reduce SREBP-1c expression in DIO mice. SREBP-1c has been reported to activate FAS and ACC promoters (Wang et al., 2015). Fatty acid synthase (FAS) can catalyze the *de novo* synthesis of fatty acids in cytoplasm (Jensen-Urstad and Semenkovich, 2012). Our results showed that the hepatic expression of FAS in DIO mouse was significantly higher than that in Con mice; *Rho* has the effect of reducing FAS protein expression, reducing *de novo* synthesis of fatty acids in liver to improve lipid accumulation in the liver. The first step, also the rate limiting step, in fatty acid biosynthesis is the reaction of ATP-dependent carboxylation of acetyl-CoA to form malonyl-CoA, and is catalyzed by acetyl-CoA carboxylase (ACC) (Tong and Harwood, 2006). In this study, the hepatic expression of ACC in DIO mice was significantly higher than that in Con mice. *Rho* has the effect of down-regulating ACC protein expression and reducing the synthesis of fatty acids.

***Rho* Decreased the *de Novo* Lipogenesis via Improving Insulin Resistance in DIO Mice**

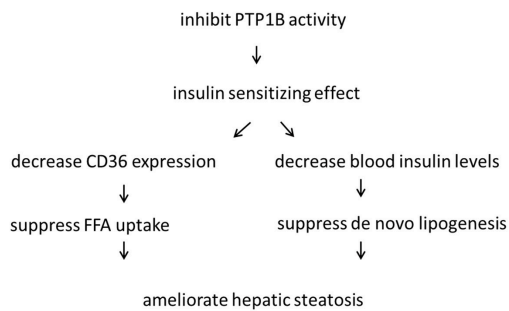
Insulin resistance plays a key role in hepatic lipid (especially fatty acids) accumulation and the subsequent increase of adipose tissue lipolysis (Bugianesi et al., 2010). In insulin resistance state, the pancreas compensates to increase the production of insulin to maintain normal glucose levels. It is reported that the higher level of insulin over-stimulates *de novo* lipogenesis, and leads to lipids accumulation based on the regulation of SREBP-1c (Shimomura et al., 2000; Konner and Bruning, 2012). As mentioned above, SREBP-1c is a key regulator in *de novo* adipogenesis (Rawson, 2003; Wang et al., 2015). Insulin is considered an important SREBP-1c activator that induces SREBP-1c expression via multiple insulin signaling pathways such as mTORC1, PI3K-AKT, and others (Wong and Sul, 2010; Shao and Espenshade, 2012; Alam et al., 2016). This indicates that improving insulin resistance may reduce the lipid synthesis and accumulation in the liver. This insulin sensitizing effect may relate to the down-regulated SREBP-1c expressions in *Rho* treatment group.

***Rho* Improved Insulin Resistance via Inhibiting PTP1B Activity in DIO Mice**

The protein tyrosine phosphatase1B (PTP1B) is a negative regulator of both insulin and leptin signaling, and shows a highly validated therapeutic target for the treatment of diabetes and obesity (Zhang and Zhang, 2007). In previous study in our lab, *Rho* was proved to have inhibitory effect on PTP1B ($IC_{50} = 0.106 \text{ mg}\cdot\text{L}^{-1}$) (Tian et al., 2016). This might contribute

to the insulin sensitizing effects of *Rho*. The mechanism of the improvement effects of *Rho* was summarized as follows:

Mechanism of the improvement effects of *Rho* on hepatic steatosis in DIO mice



Furthermore, *Rho* was observed to ameliorate hepatic microcirculation disturbances in DIO mice in this study. It might be speculated that *Rho* ameliorated the lipid accumulation in liver, and the specific mechanism needs to be further explored.

REFERENCES

- Alam, S., Mustafa, G., Alam, M., and Ahmad, N. (2016). Insulin resistance in development and progression of nonalcoholic fatty liver disease. *World J. Gastrointest. Pathophysiol.* 7, 211–217. doi: 10.4291/wjgp.v7.i2.211
- Banini, B. A., and Sanyal, A. J. (2017). Current and future pharmacologic treatment of nonalcoholic steatohepatitis. *Curr. Opin. Gastroenterol.* 33, 134–141. doi: 10.1097/MOG.0000000000000356
- Bhagavan, B. S., Wenk, R. E., McCarthy, E. F., Gebhardt, F. C., and Lustgarten, J. A. (1982). Long-term use of tetracycline. *JAMA*, 247, 2780–2780. doi: 10.1001/jama.1982.03320450018017
- Bligh, E. G., and Dyer, W. J. (1959). A rapid method of total lipid extraction and purification. *Can. J. Biochem. Physiol.* 37, 911–917. doi: 10.1139/y59-099
- Brüning, A., Brem, G. J., Vogel, M., and Mylonas, I. (2014). Tetracyclines cause cell stress-dependent ATF4 activation and mTOR inhibition. *Exp. Cell Res.* 320, 281–289. doi: 10.1016/j.yexcr.2013.11.012
- Bugianesi, E., Moscatelli, S., Ciaravella, M. F., and Marchesini, G. (2010). Insulin resistance in nonalcoholic fatty liver disease. *Curr. Pharm. Des.* 16, 1941–1951. doi: 10.2174/138161210791208875
- Calamita, G., Gena, P., Ferri, D., Rosito, A., Rojek, A., Nielsen, S., et al. (2012). Biophysical assessment of aquaporin-9 as principal facilitative pathway in mouse liver import of glucogenetic glycerol. *Biol. Cell* 104, 342–351. doi: 10.1111/boc.201100061
- Chan, S. W. (2012). *Panax ginseng*, *Rhodiola rosea* and *Schisandra chinensis*. *Int. J. Food Sci. Nutr.* 63(Suppl 1), 75–81. doi: 10.3109/09637486.2011.627840
- Chen, W. X., Wang, F., Liu, Y. Y., Zeng, Q. J., Sun, K., Xue, X., et al. (2008). Effect of notoginsenoside R1 on hepatic microcirculation disturbance induced by gut ischemia and reperfusion. *World J. Gastroenterol.* 14, 29–37. doi: 10.3748/wjg.14.29
- Cong, W. N., Tao, R. Y., Tian, J. Y., Liu, G. T., and Ye, F. (2008). The establishment of a novel non-alcoholic steatohepatitis model accompanied with obesity and insulin resistance in mice. *Life Sci.* 82, 983–990. doi: 10.1016/j.lfs.2008.01.022
- Ferre, P., and Foufelle, F. (2010). Hepatic steatosis: a role for *de novo* lipogenesis and the transcription factor SREBP-1c. *Diabetes Obes. Metab.* 12(Suppl. 2), 83–92. doi: 10.1111/j.1463-1326.2010.01275.x
- Gena, P., Mastrodonato, M., Portincasa, P., Fanelli, E., Mentino, D., Rodríguez, A., et al. (2013). Liver glycerol permeability and aquaporin-9 are dysregulated

In conclusion, our data suggest that *Rho* is a lead nature product for hepatic steatosis treatment. Its mechanism is related to improving insulin resistance, suppressing fatty acid uptake, inhibiting *de novo* lipogenesis, and could ameliorate microcirculatory disturbances in liver.

AUTHOR CONTRIBUTIONS

QY, PS, SK, JT, and XL conducted the pharmacological experiments and performed data analysis; YY and PZ prepared the active fractions from *Rhodiola crenulata* (*Rho*); JL, YL, and JH designed and conducted the experiments in hepatic microcirculation observation; XZ and FY designed the study, made data interpretation and prepared the manuscript.

ACKNOWLEDGMENTS

This work was supported by National Major Special Project on New Drug Innovation of China (No. 2009ZX09103-432; 2012ZX09103-101-063). We also thank for the support of CAMS Innovation Fund for Medical Sciences (CIFMS-2016-I2M-3-012).

in a murine model of non-alcoholic fatty liver disease. *PLoS ONE* 8:e78139. doi: 10.1371/journal.pone.0078139

- Grech-Baran, M., Sykowska-Baranek, K., and Pietrosiuk, A. (2015). Approaches of *Rhodiola kirilowii* and *Rhodiola rosea* field cultivation in Poland and their potential health benefits. *Ann. Agric. Environ. Med.* 22, 281–285. doi: 10.5604/12321966.1152081
- Gruben, N., Shiri-Sverdlov, R., Koonen, D. P., and Hofker, M. H. (2014). Nonalcoholic fatty liver disease: a main driver of insulin resistance or a dangerous liaison? *Biochim. Biophys. Acta* 1842, 2329–2343. doi: 10.1016/j.bbdis.2014.08.004
- Heaton, P., Fenwick, S., and Brewer, D. (2007). Association between tetracycline or doxycycline and hepatotoxicity: a population based case-control study. *J. Clin. Pharm. Ther.* 32, 483–487. doi: 10.1111/j.1365-2710.2007.00853.x
- Jensen-Urstad, A. P., and Semenkovich, C. F. (2012). Fatty acid synthase and liver triglyceride metabolism: housekeeper or messenger? *Biochim. Biophys. Acta* 1821, 747–753. doi: 10.1016/j.bbailip.2011.09.017
- Konner, A. C., and Brüning, J. C. (2012). Selective insulin and leptin resistance in metabolic disorders. *Cell Metab.* 16, 144–152. doi: 10.1016/j.cmet.2012.07.004
- Koonen, D. P., Jacobs, R. L., Febbraio, M., Young, M. E., Soltys, C. L., Ong, H., et al. (2007). Increased hepatic CD36 expression contributes to dyslipidemia associated with diet-induced obesity. *Diabetes* 56, 2863–2871. doi: 10.2337/db07-0907
- Lekomtseva, Y., Zhukova, I., and Wacker, A. (2017). *Rhodiola rosea* in subjects with prolonged or chronic fatigue symptoms: results of an open-label clinical trial. *Complement. Med. Res.* 24, 46–52. doi: 10.1159/000457918
- Lin, K. T., Hsu, S. W., Lai, F. Y., Chang, T. C., Shi, L. S., and Lee, S. Y. (2016). *Rhodiola crenulata* extract regulates hepatic glycogen and lipid metabolism via activation of the AMPK pathway. *BMC Complement. Altern. Med.* 16:127. doi: 10.1186/s12906-016-1108-y
- Ma, Y. M., Tao, R. Y., Liu, Q., Li, J., Tian, J. Y., Zhang, X. L., et al. (2011). PTP1B inhibitor improves both insulin resistance and lipid abnormalities *in vivo* and *in vitro*. *Mol. Cell. Biochem.* 357, 65–72. doi: 10.1007/s11010-011-0876-4
- Miquilena-Colina, M. E., Lima-Cabello, E., Sánchez-Campos, S., García-Mediavilla, M. V., Fernández-Bermejo, M., Lozano-Rodríguez, T., et al. (2011). Hepatic fatty acid translocase CD36 upregulation is associated with insulin resistance, hyperinsulinaemia and increased steatosis in non-alcoholic steatohepatitis and chronic hepatitis C. *Gut* 60, 1394–1402. doi: 10.1136/gut.2010.222844

- Orellana-Gavaldà, J. M., Herrero, L., Malandrino, M. I., Pañeda, A., Sol Rodríguez-Peña, M., Petry, H., et al. (2011). Molecular therapy for obesity and diabetes based on a long-term increase in hepatic fatty-acid oxidation. *Hepatology* 53, 821–832. doi: 10.1002/hep.24140
- Pereira, I. V., Stefano, J. T., and Oliveira, C. P. (2011). Microsomal triglyceride transfer protein and nonalcoholic fatty liver disease. *Expert Rev. Gastroenterol. Hepatol.* 5, 245–251. doi: 10.1586/egh.11.22
- Petta, S., Valenti, L., Bugianesi, E., Targher, G., Bellentani, S., Bonino, F., et al. (2016). A “systems medicine” approach to the study of non-alcoholic fatty liver disease. *Dig. Liver Dis.* 48, 333–342. doi: 10.1016/j.dld.2015.10.027
- Rawson, R. B. (2003). The SREBP pathway—insights from *Insigs* and insects. *Nat. Rev. Mol. Cell Biol.* 4, 631–640. doi: 10.1038/nrm1174
- Rodríguez, A., Catalán, V., Gómez-Ambrosi, J., and Frühbeck, G. (2006). Role of aquaporin-7 in the pathophysiological control of fat accumulation in mice. *FEBS Lett.* 580, 4771–4776. doi: 10.1016/j.febslet.2006.07.080
- Rodríguez, A., Catalán, V., Gómez-Ambrosi, J., and Frühbeck, G. (2011). Aquaglyceroporins serve as metabolic gateways in adiposity and insulin resistance control. *Cell Cycle* 10, 1548–1556. doi: 10.4161/cc.10.10.15672
- Rodríguez, A., Gena, P., Méndez-Giménez, L., Rosito, A., Valentí, V., Rotellar, F., et al. (2014). Reduced hepatic aquaporin-9 and glycerol permeability are related to insulin resistance in non-alcoholic fatty liver disease. *Int. J. Obes.* 38, 1213–1220. doi: 10.1038/ijo.2013.234
- Rodríguez, A., Marinelli, R. A., Tesse, A., Frühbeck, G., and Calamita, G. (2015). Sexual dimorphism of adipose and hepatic aquaglyceroporins in health and metabolic disorders. *Front. Endocrinol.* 6:171. doi: 10.3389/fendo.2015.00171
- Rodríguez-Ramiro, I., Vauzour, D., and Minihane, A. M. (2016). Polyphenols and non-alcoholic fatty liver disease: impact and mechanisms. *Proc. Nutr. Soc.* 75, 47–60. doi: 10.1017/S0029665115004218
- Sayiner, M., Koenig, A., Henry, L., and Younossi, Z. M. (2016). Epidemiology of nonalcoholic fatty liver disease and nonalcoholic steatohepatitis in the United States and the Rest of the World. *Clin. Liver Dis.* 20, 205–214. doi: 10.1016/j.cld.2015.10.001
- Shao, W., and Espenshade, P. J. (2012). Expanding roles for SREBP in metabolism. *Cell Metab.* 16, 414–419. doi: 10.1016/j.cmet.2012.09.002
- Shimomura, I., Matsuda, M., Hammer, R. E., Bashmakov, Y., Brown, M. S., and Goldstein, J. L. (2000). Decreased IRS-2 and increased SREBP-1c lead to mixed insulin resistance and sensitivity in livers of lipodystrophic and ob/ob mice. *Mol. Cell* 6, 77–86. doi: 10.1016/S1097-2765(05)00010-9
- Thompson, R. S., Jacques, D., Haslam, E., and Tanner, R. J. N. (1972). Plant proanthocyanidins. Part I. Introduction; the isolation, structure, and distribution in nature of plant procyranidins. *J. Chem. Soc. Perkin Trans.* 1, 1387–1399. doi: 10.1039/P19720001387
- Tian, J., Zhou, Y., Chen, L., Li, X. L., Zhang, X. L., Han, J., et al. (2016). Prescription of Jingdan insulin sensitizer for treatment of metabolic syndrome. *China J. Chin. Materia Med.* 41, 272–278. doi: 10.4268/cjcm20160218r
- Tian, J. Y., Tao, R. Y., Zhang, X. L., Liu, Q., He, Y. B., Su, Y. L., et al. (2015). Effect of *Hypericum perforatum* L. extract on insulin resistance and lipid metabolic disorder in high-fat-diet induced obese mice. *Phytother. Res.* 29, 86–92. doi: 10.1002/ptr.5230
- Tong, L., and Harwood, H. J. Jr. (2006). Acetyl-coenzyme A carboxylases: versatile targets for drug discovery. *J. Cell Biochem.* 99, 1476–1488. doi: 10.1002/jcb.21077
- Vauzour, D., Rodríguez-Ramiro, I., Rushbrook, S., Ipharraguerre, I. R., Bevan, D., Davies, S., et al. (2018). n-3 Fatty acids combined with flavan-3-ols prevent steatosis and liver injury in a murine model of NAFLD. *Biochim. Biophys. Acta* 1864, 69–78. doi: 10.1016/j.bbadis.2017.10.002
- Wang, Y., Viscarra, J., Kim, S. J., and Sul, H. S. (2015). Transcriptional regulation of hepatic lipogenesis. *Nat. Rev. Mol. Cell Biol.* 16, 678–689. doi: 10.1038/nrm4074
- Wei, W., Li, Z. P., Zhu, T., Fung, H. Y., Wong, T. L., Wen, X., et al. (2017). Anti-fatigue effects of the unique polysaccharide marker of *Dendrobium officinale* on BALB/c MICE. *Molecules*, 22(1). doi: 10.3390/molecules22010155
- Wong, R. H., and Sul, H. S. (2010). Insulin signaling in fatty acid and fat synthesis: a transcriptional perspective. *Curr. Opin. Pharmacol.* 10, 684–691. doi: 10.1016/j.coph.2010.08.004
- Wu, T., Zhou, H., Jin, Z., Bi, S., Yang, X., Yi, D., et al. (2009). Cardioprotection of salidroside from ischemia/reperfusion injury by increasing N-acetylglucosamine linkage to cellular proteins. *Eur. J. Pharmacol.* 613, 93–99. doi: 10.1016/j.ejphar.2009.04.012
- Yamamoto, T., Yamaguchi, H., Miki, H., Shimada, M., Nakada, Y., Ogino, M., et al. (2010). Coenzyme a: diacylglycerol acyltransferase 1 inhibitor ameliorates obesity, liver steatosis, and lipid metabolism abnormality in KKA y mice fed high-fat or high-carbohydrate diets. *Eur. J. Pharmacol.* 640, 243–249. doi: 10.1016/j.ejphar.2010.04.050
- Ye, F., Tao, R., Cong, W., Tian, J., and Liu, Q. (2008). Utilization of fluorescence tracer in hyperinsulinemic-euglycemic clamp test in mice. *J. Biochem. Biophys. Methods* 70, 978–984. doi: 10.1016/j.jprot.2008.01.003
- Yin, H. Q., Kim, M., Kim, J. H., Kong, G., Lee, M. O., Kang, K. S., et al. (2006). Hepatic gene expression profiling and lipid homeostasis in mice exposed to steatogenic drug, tetracycline. *Toxicol. Sci.* 94, 206–216. doi: 10.1093/toxsci/kfl078
- Zhang, S., and Zhang, Z.-Y. (2007). PTP1B as a drug target: recent developments in PTP1B inhibitor discovery. *Drug Discov. Today* 12, 373–381. doi: 10.1016/j.drudis.2007.03.011

Conflict of Interest Statement: The authors declare that the research was conducted in the absence of any commercial or financial relationships that could be construed as a potential conflict of interest.

Copyright © 2018 Yi, Sun, Li, Kong, Tian, Li, Yang, Zhang, Liu, Han, Zhang and Ye. This is an open-access article distributed under the terms of the Creative Commons Attribution License (CC BY). The use, distribution or reproduction in other forums is permitted, provided the original author(s) and the copyright owner are credited and that the original publication in this journal is cited, in accordance with accepted academic practice. No use, distribution or reproduction is permitted which does not comply with these terms.